

INVARIANT THREE AND FOUR-PHASE EQUILIBRIA IN THE Mg-RICH  
CORNER OF THE Mg-Cu-Sn TERNARY SYSTEM

E. E. Vicente<sup>1</sup>, S. Bernúdez<sup>1</sup>, A. Esteban<sup>2</sup>,  
S. Arcondo<sup>3</sup>, H. Sirkin<sup>3</sup> and R. Tendler<sup>1</sup> *orig. rel.*

<sup>1</sup>Departamento de Materiales, Comisión Nacional de  
Energía Atómica, Av. Libertador 8250, 1429 Buenos Aires,  
Argentina.

<sup>2</sup>División Tecnología de Plutonio, Comisión Nacional de  
Energía Atómica, Av. Libertador 8250, 1429 Buenos Aires,  
Argentina.

<sup>3</sup>Departamento de Física, Facultad de Ingeniería, Univer-  
sidad de Buenos Aires, Paseo Colón 850, 1063 Buenos  
Aires, Argentina.

ABSTRACT

Invariant three and four-phase equilibria in the Mg-rich corner of the Mg-Cu-Sn ternary system have been studied by differential thermal analysis, optical microscopy, electron probe microanalysis and x-ray diffraction. The  $L \rightleftharpoons \frac{1}{2}(Mg) + Mg_2Cu + Mg_2Sn$  ternary eutectic reaction was found to be at 467 °C and at Mg-13.5at%Cu-4.4at%Sn. The  $L \rightleftharpoons Mg_2Cu + Mg_2Sn$  pseudobinary eutectic reaction is tentatively located at 522 °C and at Mg-26.0at%Cu-7.7at%Sn.

## 1. INTRODUCTION

Mg-rich alloys of the Mg-Cu-Sn system had shown to be quite suitable for the development of experimental and theoretical thermodynamic studies on the glass-forming ability of ternary alloys [1,2]. More specifically, the Mg-Mg<sub>2</sub>Cu-Mg<sub>2</sub>Sn [3] ternary subsystem has a phase diagram rather simple: it is made up by the Mg-Mg<sub>2</sub>Cu [4] and the Mg-Mg<sub>2</sub>Sn [5] binary subsystems, and by the Mg<sub>2</sub>Cu-Mg<sub>2</sub>Sn [3] pseudobinary subsystem. The melting point of Mg is 650 °C [6]. Mg<sub>2</sub>Cu and Mg<sub>2</sub>Sn stoichiometric intermetallic compounds melt congruently at 568° and 770.5 °C, respectively. The Mg-Mg<sub>2</sub>Cu subsystem has an eutectic point at 14.5at%Cu and at 485 °C. The solubility of Cu in Mg is very low: 0.013at%Cu at 485 °C. The Mg-Mg<sub>2</sub>Sn subsystem has an eutectic point at 10.7at%Sn and at 561.2 °C. The maximum solubility of Sn in Mg is 3.35at%Sn at 561.2 °C [4,5].

However, the information available on the ternary system is insufficient to give details concerning the liquidus valleys and the four-phase equilibria. For instance, the pseudobinary eutectic point  $L \rightleftharpoons \text{Mg}_2\text{Cu} + \text{Mg}_2\text{Sn}$ , actually a saddle point in the ternary system, is suggested to be located at 525 °C and at Mg-25.6at%Cu-7.7at%Sn. The system is also reported to exhibit a ternary eutectic point  $L \rightleftharpoons \frac{1}{2}(\text{Mg}) + \text{Mg}_2\text{Cu} + \text{Mg}_2\text{Sn}$ , which has been provisionally located at Mg-11.4at%Cu-3.2at%Sn, but its temperature has not been measured [3]. (Mg) stands for the terminal solid solution. The above values of composition have been estimated from the phase diagram of [3].

In this work we have measured the composition and the temperature of both the ternary and the pseudobinary eutectic reactions.

## 2. EXPERIMENTAL

Two alloys of the following nominal compositions were prepared: A) Mg-11.4at%Cu-3.2at%Sn and B) Mg-25.6at%Cu-8.0at%Sn. Starting materials were Mg, Cu and Sn of 99.99% purity. The alloys (A: 0.5099 g and B: 0.6679 g) were melted at 800 °C during 30 min in nuclear grade graphite crucibles ( $\approx$  1 g each) in an electric resistance furnace under static Ar atmosphere ( $\approx$  3 atm) of 99.996% purity. A weight loss of 3.43 % for the alloy A and 1.08 % for the alloy B was observed.

Simultaneous differential thermal analysis (DTA) and thermogravimetry (TG) were performed in a Mettler Vacuum Thermoanalyzer equipment, under static atmosphere ( $\approx$  1 atm) of Ar 99.998% pure, and in the same crucibles which had been previously used for the preparation of the alloys. An empty graphite crucible was chosen as the reference "sample". The heating/cooling rates were: 6 °C/min (25-436 °C) and 1 °C/min (436-500 °C) for the alloy A, and 6 °C/min (25-507 °C) and 1 °C/min (507-556 °C) for the alloy B. After the last measurement in each alloy they were heated up to 507 °C (alloy A) and 557 °C (alloy B). Next, the furnace of the DTA-TG equipment was turned-off and the samples were allowed to cool inside the furnace down to room temperature at a rate of about 6 °C/min. Weight losses of the crucibles containing the alloys during the DTA-TG experiments were negligible ( $\approx$  0.01%). The Pt/Pt-10%Rh thermocouple was calibrated "in situ" against high-purity 99.995% In, 99.99% Al and Ag, and 99.999% Sn and Zn.

The solidification structures, after the DTA-TG experiments, were examined by optical microscopy in cross-sections at the top, center and bottom of the ingots. The specimens were prepared for microscopic examination by grinding without any lubricant on a Buheler microcut paper

sheet 600 grit soft, followed by mechanical polishing on a Mol-Struers cloth with 3  $\mu\text{m}$  diamond paste lubricated with ethylene-glycol. Then, the samples were chemically etched by immersion, stirring for 6 sec in a solution of picric acid, ethanol and water (6 g:10 ml:90 ml). Finally, they were washed and rinsed with anhydrous ethanol (water was specially avoided to prevent oxidation). The phases were identified by their colours under the light microscope and by electron probe microanalysis (EPMA) in a Cameca SX 50 equipment outfitted with a wave-length-dispersive spectrometer. In order to improve the accuracy of the composition measurements, the specimens for EPMA were polished but unetched. In spite of the fact that the samples were unetched very good secondary electrons images were achieved. The phases were also identified by x-ray diffraction (XRD) in a Phillips PW 1400 equipment employing graphite monochromatized  $\text{Co}_K\alpha$  radiation.

### 3. RESULTS

Both alloys show off-eutectic microstructures (Figs. 1-6). The bottom of the alloy A has elongated colonies of the (Mg)- $\text{Mg}_2\text{Cu}$  binary eutectic in a fine, ground matrix of the (Mg)- $\text{Mg}_2\text{Cu}$ - $\text{Mg}_2\text{Sn}$  ternary eutectic (Fig. 1). Towards the top of the ingot non-faceted, <sup>Figures 1, 2 and 3</sup> primary dendrites of (Mg) were also observed (Fig. 2). Primary (Mg) certainly segregated upward by gravity during the freezing of this alloy. The morphology of the binary eutectic is nearly lamellar and that of the ternary one seems to be fibrous or rod-like, being both  $\text{Mg}_2\text{Cu}$  and  $\text{Mg}_2\text{Sn}$  compounds partially surrounded by (Mg) (Fig. 3). The interlamellar spacing of the binary eutectic ranges between 5 and 10  $\mu\text{m}$ , and the interrod spacing of the ternary eutectic is approximately 2  $\mu\text{m}$ . Twelve measurements of composition performed by EPMA on 15x15  $\mu\text{m}$  scanned areas on the finest ternary eutectic

zones resulted in the following average value: Mg-12.5at%Cu-4.4at%Sn, which is slightly different from the one reported in [3]. Standard deviations in composition were: 0.5at%Mg, 0.4at%Cu and 0.3at%Sn. EPMA performed in five different dendrites of (Mg) gave an average composition of Mg-1.5at%Sn-0.05at%Cu. The thermogram of this alloy (Fig. 7) shows only one peak at 467 °C, as measured on the initial deviation from the base line [7], during both melting and solidification, which is attributable to the ternary eutectic reaction. No primary arrest was observed.

The sample B exhibits a honeycomb pattern of colonies (sometimes termed "grains") of the Mg<sub>2</sub>Cu-Mg<sub>2</sub>Sn pseudobinary eutectic (Fig. 4). The size of the cells ranges between 100 and 500 μm. This eutectic has <sup>Figures 4, 5 and 6</sup> a mixed lamellar-rodlike morphology, being Mg<sub>2</sub>Cu the major phase (Fig. 5). The size of the interrod or interlamellar spacing is about 1 to 2 μm at the center of the colonies. In addition, the specimen has very few, isolated, faceted, primary crystals of Mg<sub>2</sub>Sn, and also small amounts of an intercellular, three-phase assemblage that resembles a ternary eutectic (Fig. 6). It includes Mg<sub>2</sub>Cu, Mg<sub>2</sub>Sn and a reddish (as view on unetched metallographic surfaces) third phase, this colour indicating the presence of a higher Cu content. The average composition of this assemblage could not be suitably measured by EPMA. The XRD pattern shows the existence of only Mg<sub>2</sub>Cu and Mg<sub>2</sub>Sn phases. The Cu-rich phase could not be detected by XRD because there is only a small percentage of it in the whole sample. Six measurements of composition carried out by EPMA on 15x15 μm scanned areas on the finest pseudobinary eutectic regions resulted in the following average value: Mg-26.0at%Cu-7.7at%Sn, which closely agrees with the one reported in [3]. Standard deviations in composition were: 0.1at%Mg, 0.2at%Cu and 0.07at%Sn. The thermogram of this alloy (Fig. 7) exhibits two peaks: a large one at 522 °C that is ascribable to the pseudobinary eutectic reac-

tion, and a very small one at 463 °C that could not be assigned to any reported invariant reaction. The  $\text{Mg} + \text{Mg}_2\text{Cu} + \text{Mg}_2\text{Sn}$  ternary eutectic reaction was ruled out by both metallography and DTA. No primary arrest was observed. The main arrest is rounded at the beginning point upon heating and at the ending point upon cooling, then suggesting that the invariant three-phase equilibrium (the pseudobinary reaction) was not strictly attained [7]. The difference between the temperature of the main peak measured during solidification and that measured during melting is 0.5 °C. The pseudobinary eutectic temperature is just 3 °C below the reported one in [3].

Fig. 7

#### 4. DISCUSSION

Both, the previously published liquidus projection [3], and the liquidus projection that is proposed in the present work for the Mg-Mg<sub>2</sub>Cu-Mg<sub>2</sub>Sn ternary subsystem, are shown in Fig. 8. The last one was plotted using the assessed binary phase diagrams [4,5], the pseudobinary eutectic point reported in [3] and the ternary eutectic point measured in this work. Because of the lack of data, the field boundaries, which are the eutectic valleys, have been tentatively drawn as straight lines.

The weight losses that occurred on melting alloys A and B have to be mainly attributed to the vaporization of Mg, because this is the volatile component [8]. On account of these Mg losses, the corrected compositions become Mg-12.2at%Cu-3.5at%Sn for the alloy A, and Mg-26.1at%Cu-8.1at%Sn for the alloy B (points A' and B', respectively, in Fig. 8).

The observed microstructure of the sample A and its corrected composition lack consistency [9] if the last is

located on the previously estimated phase diagram [3]. Instead, the microstructure is consistent with the corrected composition when this is placed on the phase diagram proposed in this work. In fact, the alloy A' lies within the primary phase field of (Mg) of the here proposed phase diagram, and within the angle delimited by the Mg-Cu binary system and by the straight line joining the Mg corner and the (Mg)-Mg<sub>2</sub>Cu-Mg<sub>2</sub>Sn ternary eutectic point (Fig. 8). The solidification path [10, 11] of this alloy is quite simple. On cooling from the melt, initial crystallization of primary (Mg) occurs at some unknown liquidus temperature. Primary arrest in the thermogram of the sample A is missed probably because its liquidus temperature is above 500 °C. Let us assume that pure Mg instead of (Mg) precipitates. Then, the composition of its complementary liquid moves along the extension of line Mg-A' away from Mg. When the Mg-Mg<sub>2</sub>Cu eutectic valley is reached ( $467\text{ }^{\circ}\text{C} < T < 485\text{ }^{\circ}\text{C}$ ) this eutectic begins to solidify. From this point the composition of the liquid runs along this eutectic valley towards the Mg-Mg<sub>2</sub>Cu-Mg<sub>2</sub>Sn ternary eutectic point. The crystallization ends at the quaternary invariant point E (467 °C), where the remainder of the liquid isothermally transforms into the ternary eutectic. Because (Mg) instead of pure Mg is actually the primary phase, the first step of the solidification path is not a straight line, but a curve. There are not enough data on the solubility of Sn and Cu in (Mg), except a rough estimation at 400 °C [3]. However, from the binary phase diagrams [4, 5] and from our measurements of composition in primary (Mg), we can state that Sn is more soluble in (Mg) than Cu. In addition, the solubility of Sn in (Mg) decreases from 2.4at% at 500 °C to 1.8at% at 465 °C for Mg-Sn binary alloys [5]. Therefore, the first step of the solidification path of the sample A should be slightly convex (as viewed from the Mg-Cu binary system), but it will certainly run towards the (Mg)-Mg<sub>2</sub>Cu eutectic valley. The equilibrium reactions that occurred

upon cooling of the sample A can be summarized as follows:  
 $L \rightarrow L + (Mg) \rightarrow L + (Mg) + Mg_2Cu \rightarrow (Mg) + Mg_2Cu + Mg_2Sn$ .

Both the nominal and the corrected composition of the sample B lie within the primary phase field of  $Mg_2Sn$ , very close to the  $Mg_2Cu$ - $Mg_2Sn$  field boundary, but slightly shifted from the pseudobinary section towards the  $(MgCu_2)$ - $Mg_2Cu$ - $Mg_2Sn$  ternary subsystem proposed in [3].  $(MgCu_2)$  stands for the solid solution of Cu, Mg and Sn in  $MgCu_2$ . Then, the equilibrium reactions that occurred upon cooling of the sample B could be summarized as follows:  $L \rightarrow L + Mg_2Sn \rightarrow L + Mg_2Sn + Mg_2Cu \rightarrow Mg_2Sn + Mg_2Cu + (MgCu_2)$ . The microstructure of the sample B is consistent with such reactions. However, the solidification path for the alloy B', for instance, should end at the  $L \rightarrow (MgCu_2) + Mg_2Cu + Mg_2Sn$  ternary eutectic point tentatively located at Mg-27.6at%Cu-8.4at%Sn and at 520 °C [3]. The small arrest at 463 °C measured in the thermogram of the sample B, suggests a different temperature for this ternary eutectic reaction or the existence of other non reported invariant reaction. On the other hand, for Mg-Cu and Mg-Sn binary systems the liquidus lines show no discontinuities at the congruent points of  $Mg_2Cu$  and  $Mg_2Sn$  intermetallic compounds, but they form maxima with horizontal tangents and hence they are mathematically continuous. Likewise, the liquidus surfaces of the ternary system show no discontinuities when they cross the pseudobinary cut [12]. Furthermore, the field boundary which is the intersection of two liquidus surfaces ( $L + Mg_2Cu$  and  $L + Mg_2Sn$ ) has an horizontal tangent (a maximum temperature of equilibrium among these three phases at the saddle point) [10]. These considerations permit us to state that the temperature of the pseudobinary eutectic reaction measured in this work should be slightly below the "true" temperature of the saddle point. Hence, the results presented in Fig. 8 are provisional and more careful experiments are needed to establish this region of the phase

diagram.

## 5. CONCLUSIONS

The  $L \rightleftharpoons (Mg) + Mg_2Cu + Mg_2Sn$  ternary eutectic reaction was found to be at 467 °C and at Mg-13.5at%Cu-4.4at%Sn. The  $L \rightleftharpoons Mg_2Cu + Mg_2Sn$  pseudobinary eutectic reaction is tentatively located at 522 °C and at Mg-26.0at%Cu-7.7at%Sn.

## ACKNOWLEDGMENTS

The authors are grateful to Dr. J. P. Abriata for stimulus and discussions, to Dr. G. Vigna for leading the performance and interpretation of EPMA, and to Mr. R. Gonzalez for performing the EPMA.

## REFERENCES

1. H. SIRKIN, N. MINGOLO, E. NASSIF and B. ARCONDO, *J. Non-Cryst. Solids* 93 (1987) 323.
2. F. SOMMER, M. FRIPAN and B. PREDEL, in *Proceedings of the 4th International Conference on Rapid Quenched Metals*, Sendai (Japan), August 1981, edited by T. Masumoto and K. Suzuki (The Japan Institute of Metals, Sendai, 1982) p. 209.
3. Y. A. CHANG, J. P. NEUMANN, A. MIKULA and D. GOLDBLANK, *National Standard Reference Data System*, National Bureau of Standards, USA (1979) 520.
4. A. A. NAYEB-HASHEMI and J. B. CLARK, *Bull. Alloys Phase Diagrams* 5 (1984) 36 and 103.
5. A. A. NAYEB-HASHEMI and J. B. CLARK, *Bull. Alloys Phase Diagrams* 5 (1984) 466 and 535.
6. "Melting point of the elements", *Bull. Alloys Phase Diagrams* 7 (1986) 601.
7. R. D. SHULL, *Bull. Alloys Phase Diagrams* 4 (1983) 5.
8. "Vapour pressure of the elements", in *Handbook of Chemistry and Physics*, edited by R. C. Weast (CRC Press, Florida, 1978) p. D-258.
9. D. G. MACCARTNEY, J. D. HUNT and R. M. JORDAN, *Metall. Trans.* 11A (1980) 1243.
10. F. N. RHINES, in *Phase Diagrams in Metallurgy* (McGraw-Hill, New York, 1956) pp. 159 and 163.

11. G. D. PELTON, in "Physical Metallurgy", edited by R. W. Cahn and P. Haasen (Elsevier, Amsterdam, 1963) p. 327.
12. G. MASSING, in "Ternary Systems", (Reinhold, New York, 1944) p. 42.

## FIGURE CAPTIONS

- Fig. 1: Optical micrograph of the alloy A, as-cast. Colonies of the (Mg)-Mg<sub>2</sub>Cu binary eutectic in a matrix of the (Mg)-Mg<sub>2</sub>Cu-Mg<sub>2</sub>Sn ternary eutectic. (Mg): gray, Mg<sub>2</sub>Cu: white, Mg<sub>2</sub>Sn: black. Magnification 200 times.
- Fig. 2: Idem Fig. 1. Zone showing primary dendrites of (Mg). Magnification 100 times.
- Fig. 3: Idem Fig. 1. Magnification 1000 times.
- Fig. 4: Optical micrograph of the alloy B, as-cast. Colonies of the Mg<sub>2</sub>Cu-Mg<sub>2</sub>Sn pseudobinary eutectic, and primary crystals of Mg<sub>2</sub>Sn. Mg<sub>2</sub>Cu: white, Mg<sub>2</sub>Sn: black. Magnification 120 times.
- Fig. 5: Idem Fig. 4. Magnification 1000 times.
- Fig. 6: Idem Fig. 4. Zone showing intercellular three-phase assemblage. Mg<sub>2</sub>Cu: white, Mg<sub>2</sub>Sn: black, Cu-rich phase: gray. Magnification 570 times.
- Fig. 7: Thermograms of alloys A and B.
- Fig. 8: Liquidus projection of the Mg-Mg<sub>2</sub>Cu-Mg<sub>2</sub>Sn ternary subsystem. A and A' are the nominal and the corrected compositions of the alloy A, respectively. A and E are the reported [3] and the measured (this work) composition of the ternary eutectic, respectively. B and B' are the nominal and the corrected compositions of the alloy B, respectively. P and P' are the reported [3] and the measured (this work) compositions of the pseudobinary eutectic, respectively.

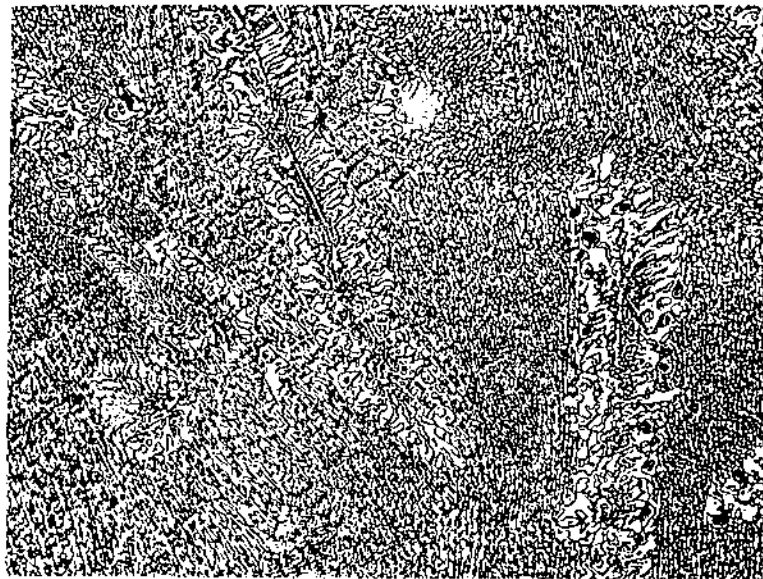


Fig. 1



Fig. 2

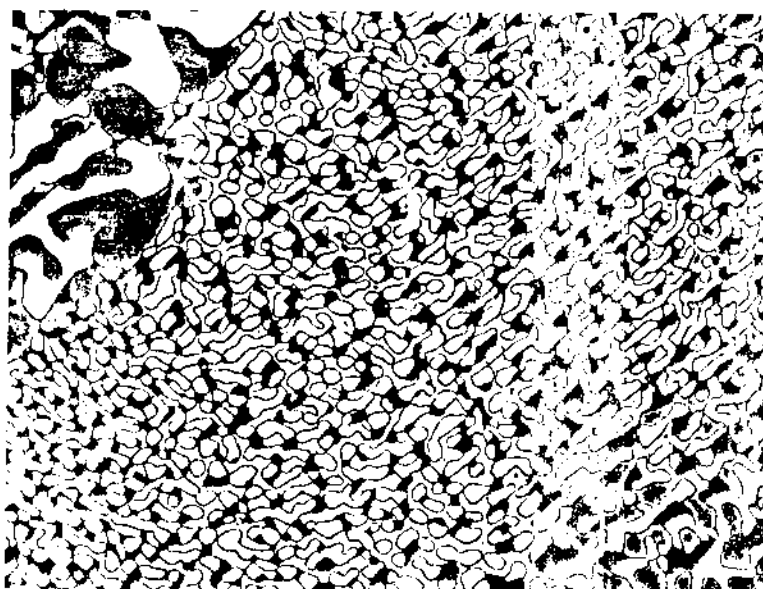


Fig. 3



Fig. 4

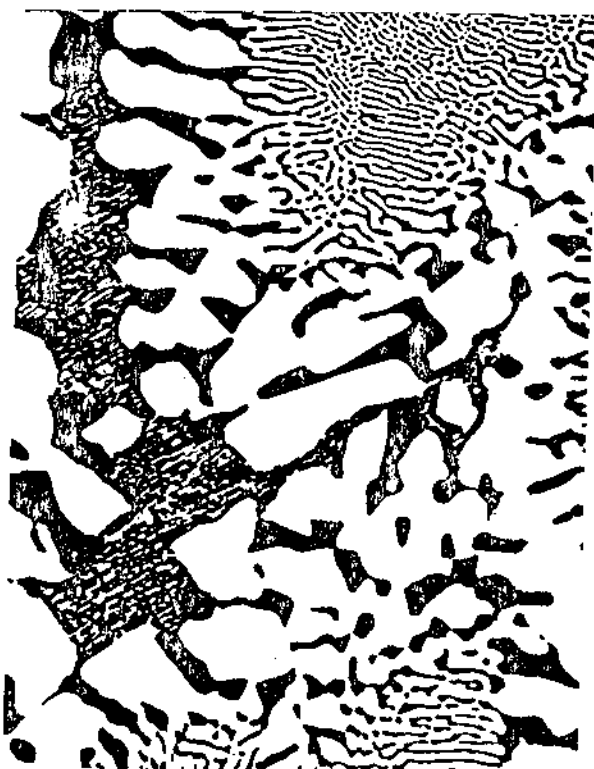


Fig. 5

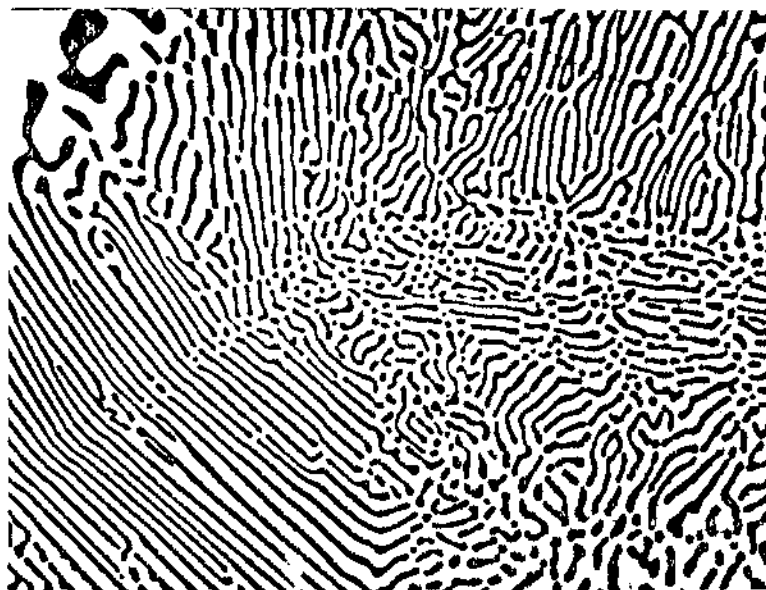


Fig. 6

Fig 7

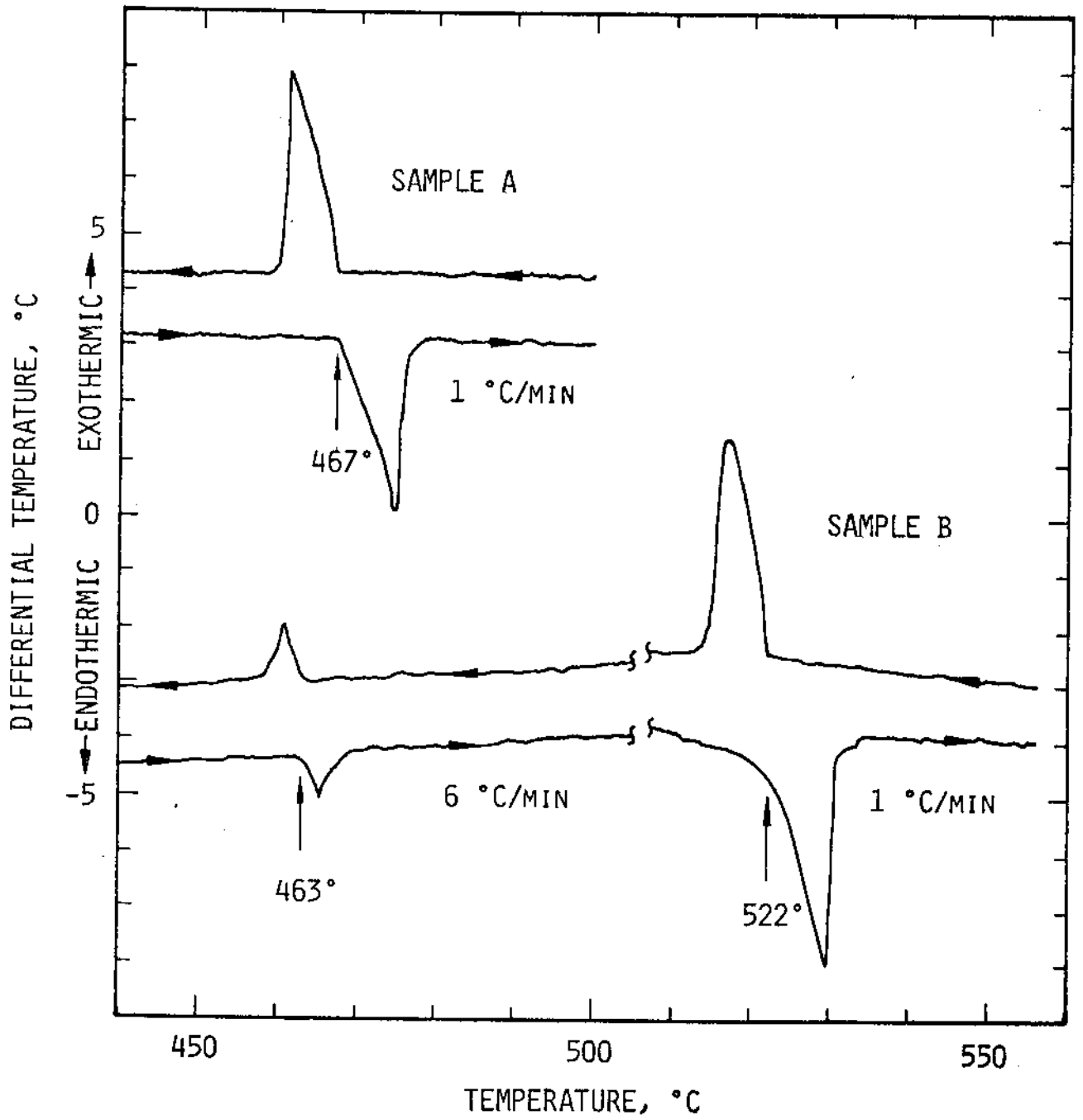


Fig. 8

